Available online at www.sciencedirect.com
ScienceDirect
Journal of Sound and Vibration 317 (2008) 127–141
JOURNAL OF SOUND AND VIBRATION
www.elsevier.com/locate/jsvi

Determination of the axial force on stay cables accounting for their bending stiffness and rotational end restraints by free vibration tests

Marcelo A. Ceballos*, Carlos A. Prato

Department of Structures, National University of Córdoba, Av. Vélez Sarsfield 1611, X5016GCA, Córdoba, Argentina

Received 4 August 2007; received in revised form 26 February 2008; accepted 27 February 2008
Handling Editor: P. Davies
Available online 9 April 2008

Abstract

Determination of the axial force in terms of its natural frequencies may be significantly influenced by the bending stiffness of the cable and the rotational elastic restraints at the ends, depending on the geometrical and mechanical parameters of the cable and its supports and restraints, particularly in cement-grouted parallel-bundle wire cables. The paper presents an explicit analytical expression for the natural frequencies taking into account both the bending stiffness of the cable and the rotational restraint at the ends that may be used to determine the axial force. While the bending stiffness of the cable and the axial force are selected as variables to attain an optimal match between analytical and experimental data, the rotational stiffness at the ends is treated as a known parameter in that process. The degree of rotational restraint at the ends cannot be accurately inferred from the sequence of the experimentally determined natural frequencies, since this parameter does not appreciably affect the progression of their values. Techniques are discussed that allow approximate determination of the rotational stiffness at the ends for the most common arrangements of anchors and cables with, and without, intermediate supports provided by deviators located near the ends. The axial force and the bending stiffness of the cable are both simultaneously adjusted by matching the natural frequencies of the analytical model with the experimental values. The proposed approach leads to a reduction of the error in the estimation of the axial force for short cables with relatively high bending stiffness such as those typical of cement-grouted parallel-bundle wire cables often used as cable stays for bridges until the early 1990s.

1. Introduction

Experimental determination of the axial force acting on cables has been found particularly useful in the safety evaluation of the cables of existing bridges. Unexpected changes in their natural frequencies have been found to originate in the loss of axial stiffness associated with the rupture of wires of their cross section, leading to a redistribution of the axial forces among adjacent cables. The present work is concerned with the interpretation of free vibration tests often performed on cables in order to measure their axial force

*Corresponding author. Tel./fax: +54 351 4334144.
E-mail addresses: mceballo@efn.uncor.edu (M.A. Ceballos), cprato@efn.uncor.edu (C.A. Prato).

0022-460X/$ - see front matter © 2008 Elsevier Ltd. All rights reserved.
doi:10.1016/j.jsv.2008.02.048

considering the elastic rotational restraints at their ends in a way that remains accurate even when the natural frequencies of the cables are significantly affected by their bending stiffness.

Determination of the axial force acting on cable stays through the analysis of free vibration records is based on the optimal selection of the parameters of an analytical model of the cables that matches the measured fundamental frequency, or frequencies, of the cable. The basic tools in this process are on one side the analytical model of the cable and its supports, and on the other side the experimental vibration records. Several technical papers have been proposed in the past to address this problem in various ways depending on the selection of the model parameters and on the experimental procedure used to collect the basic data. Among them, Casas [1] has used an experimental setup whereby the fundamental mode of vibration of the cable is excited by rhythmically oscillating a hanging weight in the vertical plane of the cable at a frequency close to the fundamental one so as to produce significant response in that mode, and the axial force acting on the cable is derived from the expression of the fundamental frequency of an ideal string, i.e. a cable with zero bending stiffness, zero sag and infinite axial stiffness. The model parameters are the mass per unit length, the cable free length and the axial force on the cable. This author proposed an optimization process that determines the best estimate of the axial force by combining the data from free vibration records with those given by strain-gauges and direct measurements of the axial force by hydraulic jacks. This approach was aimed at taking into account the uncertainties of the cable free length defined by dampers and restraining elastic collars near the ends of the cables. The inherent shortcomings of this ''combined'' approach are associated with the practical issues of carrying out strain and force readings to complement the vibration records.

In the paper of Ren et al. [2] empirical expressions to estimate cable tension based only on the cable fundamental frequency were proposed as a linearization of energy methods accounting for the influence of cable sag and bending stiffness. The main practical limitation of this approach lies in the difficulties to measure the fundamental frequency and to take into account at the same time the bending stiffness and the cable sag. As discussed in more detail in a further section, the cable sag has limited effect in the lower frequencies of the cable in the vertical plane of the cable, but no influence in the frequencies associated with displacements normal to that plane.

More recently, Smith and Johnson [3], and Smith and Campbell [4], have proposed to use for this purpose records of wind- and traffic-induced cable oscillations collected near the ends of the cables in the vertical plane of the cable, which are often of much larger amplitude than those normal to that plane. The fundamental frequency is then determined through the weighted average of the difference between the frequencies of the two consecutive higher modes, and the axial force is calculated by means of the expression for the ideal string.

A more recent paper by Geier et al. [5] proposed the simultaneous adjustment of the fundamental frequency of the cable assumed as an ideal string, and the bending stiffness of the cable that modifies the uniform interval between the successive natural frequencies through a dispersion effect. They derive the axial force from the expression of the fundamental frequency of an ideal string, where that frequency is obtained taking into account 20–25 frequencies identified from wind- and traffic-induced vibrations in the vertical plane of the cable near the ends. In this process, these authors assumed either hinged or fixed end conditions for the cables, thus not allowing for intermediate values of the end restraints. If the actual rotational stiffness at the ends is not known, the axial force determined from the experimental frequencies may be significantly affected by this parameter, and the axial force obtained from the assumption of free or fixed rotations at the supports may appreciably depart from its true value depending on the assumption adopted, especially when the cable is relatively short and has high bending stiffness typical of parallel-bundle wire cables encased in mortar-grouted PE pipes that were often used up to the 1990s in cable-stayed bridges [6]. The axial force acting on the original parallel-bundle wire cables of the Zárate-Brazo Largo Bridges described in earlier work by Prato and Ceballos [7] has been found to vary more than 10 percent depending on whether fixed or free rotations are assumed at the ends thus bringing into attention the need to account for the actual rotational stiffness at the ends.

In this paper a procedure to obtain the axial force by simultaneous adjustment of the force and bending stiffness to 20–25 experimentally identified frequencies is presented. The vibration records are obtained by recording the horizontal acceleration response due to a hand-applied impulse normal to the vertical plane of the cable at a point near the bottom end at a known distance from the end restraints. This is found to be a good choice to reduce as much as possible the influence of the assumption that the cable is axially rigid and

without sag, as assumed in evaluation of the natural frequencies with the analytical model, and to reduce the coupling of wind- and traffic-induced vibrations with the test results.

As mentioned earlier, to obtain improved accuracy in the axial force, an estimation of the rotational stiffness at the cable ends is required. This cannot be achieved only on the basis of the values of the natural frequencies since their progression is not sensitive to that parameter and a special technique is needed. For cables without intermediate supports the rotational stiffness is essentially frequency independent and may be experimentally estimated by detecting the lowest mode for which the accelerometer located at a known distance from the cable end has the smallest (zero, or near-zero) spectral amplitude in the tests. Since the experimental signals used in the analysis are associated with an applied impulse, the intensity of the test impulse to attain an acceptable noise/signal ratio may be adjusted for that purpose. For cables with intermediate supports such as those provided by collars or deviators, the rotational stiffness is frequency dependent and may be analytically estimated in terms of the distance between the intermediate support and the cable end, the axial force and the bending stiffness of the cable. The free length adopted for the analytical model of the cable is the distance between the intermediate supports and an iterative adjustment procedure is needed since the axial force is both a required parameter and also the final result of the analysis.

2. Dynamics of a cable with bending stiffness

A basic assumption in the foregoing analysis of the test data is that the cable sag does not have a significant influence on the measured frequencies of the cable. This assumption, supported by a parametric analysis presented at the end of this section, is applicable when the test excitation is applied normal to the vertical plane of the cable. The experimental procedure aims at determining the frequencies in the range of the 5th to the 20th mode, rather than the fundamental mode.

2.1. Determination of the natural frequencies

The governing differential equation for the free vibrations of a straight cable according to Clough and Penzien [8] is

$$EI\,u^{\mathrm{iv}}(x)\,y(t) - N\,u''(x)\,y(t) + m\,u(x)\,\ddot{y}(t) = 0, \tag{1}$$

where EI is the bending stiffness of the cable, N is the axial force acting on the cable and m is the mass per unit length of cable. Superscript $(')$ denotes differentiation with respect to x, and $(\dot{})$ differentiation with respect to time t. Substituting $y(t) = \mathrm{e}^{\mathrm{i}\omega t}$ and simplifying one arrives at

$$EI\,u^{\mathrm{iv}}(x) - N\,u''(x) - m\,\omega^2\,u(x) = 0. \tag{2}$$

The modal shapes of the cable are obtained in the form

$$u(x) = D_1\,\sin(\delta x) + D_2\,\cos(\delta x) + D_3\,\sinh(\varepsilon x) + D_4\,\cosh(\varepsilon x), \tag{3}$$

where

$$\delta = \sqrt{\sqrt{a^4 + g^4} + g^2}, \tag{4a}$$

$$\varepsilon = \sqrt{\sqrt{a^4 + g^4} - g^2}, \tag{4b}$$

and

$$a^4 = \frac{m\omega^2}{EI}, \tag{5a}$$

$$g^2 = -\frac{N}{2EI}. \tag{5b}$$

A suitable description of the boundary conditions imposed on the anchorage devices is obtained through rotational springs with constants K_A and K_B acting in the cable ends. The degree of fixity in the supports can

be represented through the non-dimensional parameters k_A and k_B defined as

$$k_A = \frac{K_A L}{K_A L + \pi^4 EI} \quad \text{therefore } \frac{K_A}{EI} = \frac{\pi^4}{L}\frac{k_A}{(1-k_A)}, \tag{6a}$$

$$k_B = \frac{K_B L}{K_B L + \pi^4 EI} \quad \text{therefore } \frac{K_B}{EI} = \frac{\pi^4}{L}\frac{k_B}{(1-k_B)}, \tag{6b}$$

where L is the length of the cable. The boundary conditions used to determine the constants D_1 through D_4 from Eq. (3) are

$$u_0 = 0 \quad \text{therefore } D_2 + D_4 = 0, \tag{7a}$$

$$u_L = 0 \quad \text{therefore } D_1 \sin(\delta L) + D_2 \cos(\delta L) + D_3 \sinh(\varepsilon L) + D_4 \cosh(\varepsilon L) = 0, \tag{7b}$$

$$K u_0' = EI u_0'' \quad \text{therefore } \pi^4 k_A(\delta D_1 + \varepsilon D_3) + L(1-k_A)(\delta^2 D_2 - \varepsilon^2 D_4) = 0, \tag{7c}$$

$$\begin{aligned} K u_L' = -EI u_L'' \quad \text{therefore } & \pi^4 k_B \begin{pmatrix} \delta D_1 \cos(\delta L) - \delta D_2 \sin(\delta L) \\ \quad + \cdots + \varepsilon D_3 \cosh(\varepsilon L) + \varepsilon D_4 \sinh(\varepsilon L) \end{pmatrix} \\ & + \cdots + L(1-k_B) \begin{pmatrix} -\delta^2 D_1 \sin(\delta L) - \delta^2 D_2 \cos(\delta L) \\ \quad + \cdots + \varepsilon^2 D_3 \sinh(\varepsilon L) + \varepsilon^2 D_4 \cosh(\varepsilon L) \end{pmatrix} = 0. \end{aligned} \tag{7d}$$

The natural frequencies are obtained from the condition that the determinant of the boundary conditions is set equal to zero:

$$\det\left(\begin{bmatrix} 0 & \sin(\delta L) & \pi^4 k_A \delta & \pi^4 k_B \delta \cos(\delta L) - L(1-k_B)\delta^2 \sin(\delta L) \\ 1 & \cos(\delta L) & L(1-k_A)\delta^2 & -\pi^4 k_B \delta \sin(\delta L) - L(1-k_B)\delta^2 \cos(\delta L) \\ 0 & \sinh(\varepsilon L) & \pi^4 k_A \varepsilon & \pi^4 k_B \varepsilon \cosh(\varepsilon L) + L(1-k_B)\varepsilon^2 \sinh(\varepsilon L) \\ 1 & \cosh(\varepsilon L) & -L(1-k_A)\varepsilon^2 & \pi^4 k_B \varepsilon \sinh(\varepsilon L) + L(1-k_B)\varepsilon^2 \cosh(\varepsilon L) \end{bmatrix}^{\mathrm{T}} \right) = 0. \tag{8}$$

Expanding Eq. (8) and dividing by $\cosh(\varepsilon L)$ one arrives at

$$\begin{aligned} & \pi^4 L(k_A + k_B - 2k_A k_B)(\delta^2 + \varepsilon^2)[\varepsilon \sin(\delta L) - \delta \cos(\delta L) \tanh(\varepsilon L)] \\ & \quad + \cdots + [L^2(1 - k_A - k_B + k_A k_B)(\delta^2 + \varepsilon^2)^2 - \pi^8 k_A k_B(\delta^2 - \varepsilon^2)] \sin(\delta L) \tanh(\varepsilon L) \\ & \quad + \cdots + 2\pi^8 k_A k_B \delta\varepsilon[\operatorname{sech}(\varepsilon L) - \cos(\delta L)] = 0. \end{aligned} \tag{9}$$

Parameter εL is obtained such that

$$\varepsilon L \geqslant \sqrt{n^2\pi^2 + 1/\beta^2}, \tag{10}$$

where

$$\beta = \frac{1}{L}\sqrt{\frac{EI}{N}} \tag{11}$$

is a non-dimensional form of the bending stiffness. The parameter β is the inverse of ξ defined by Geier et al. in [5]. The equality condition in Eq. (10) is only attained for the doubly hinged condition ($k_A = k_B = 0$), while for typical bending stiffness ($\beta < 0.03$) one may assume

$$\tanh(\varepsilon L) = 1, \tag{12a}$$

$$\operatorname{sech}(\varepsilon L) = 0. \tag{12b}$$

Under these assumptions, Eq. (9) takes on the form

$$\pi^4 L(k_A + k_B - 2k_A k_B)(\delta^2 + \varepsilon^2)[\varepsilon \sin(\delta L) - \delta \cos(\delta L)] - 2\pi^8 k_A k_B \delta\varepsilon \cos(\delta L) + \cdots + [L^2(1 - k_A - k_B + k_A k_B)(\delta^2 + \varepsilon^2)^2 - \pi^8 k_A k_B(\delta^2 - \varepsilon^2)] \sin(\delta L) = 0. \quad (13)$$

Re-arranging terms, one arrives at

$$A \sin(\delta L) + B \cos(\delta L) = 0, \quad (14)$$

where

$$A = \pi^8 k_A k_B(\delta^2 - \varepsilon^2) - L^2(1 - k_A - k_B + k_A k_B)(\delta^2 + \varepsilon^2)^2 - \pi^4 L(k_A + k_B - 2k_A k_B)(\delta^2 + \varepsilon^2)\varepsilon, \quad (15a)$$

$$B = 2\pi^8 k_A k_B \delta\varepsilon + \pi^4 L(k_A + k_B - 2k_A k_B)(\delta^2 + \varepsilon^2)\delta. \quad (15b)$$

Eq. (14) may also be expressed in the form

$$\rho \sin(\delta L + \theta) = 0, \quad (16)$$

where

$$\rho = \sqrt{A^2 + B^2}, \quad (17a)$$

$$\theta = \operatorname{atan}(B/A). \quad (17b)$$

Then

$$\delta L + \theta = n\pi \quad \text{with } n = 0, 1, 2, \ldots, \infty. \quad (18)$$

The value ω_n of the natural frequency of mode n of the cable may then be obtained from the parameter δ in Eq. (18) using Eqs.(4) and (5), aside the fact that θ_n is also a function of ω_n through δ and ε according to Eqs. (17b), (15), (4) and (5), by means of the following expression:

$$\omega_n = 2\pi f_n = \frac{(n\pi - \theta_n)}{L}\sqrt{\frac{N}{m}}\sqrt{1 + \beta^2(n\pi - \theta_n)^2}. \quad (19)$$

Eq. (19) provides an explicit expression for the natural frequencies of the cable in terms of parameter θ_n that is found to be convenient for practical applications in an iterative mode. Parameter θ_n becomes zero for the hinged end condition ($k_A = k_B = 0$), so that no iterations are needed in that case. For $k_A \neq 0$ and/or $k_B \neq 0$ the iterations start with the calculation of the natural frequency of mode n with Eq. (19) for $\theta_n = 0$. With such initial value of this frequency, Eqs. (4), (5), (15) and (17b) are used to calculate an approximation of θ_n, which in turn is used to calculate again ω_n from Eq. (19), thus completing the cycle of iteration to be repeated until the desired accuracy is attained. Eq. (19) remains accurate even for high bending stiffness values ($\beta \approx 0.03$) unlike the approximate expression proposed in Ref. [5] to obtain the natural frequencies of cables assuming fixed rotations at the ends, which may lead to errors higher than 10 percent for frequencies higher than the 20th mode when the non-dimensional bending stiffness is $\beta = 0.02$ or larger.

2.2. Sag effect on cable frequencies

To illustrate the effect of the sag of the cable on the natural frequencies of a typical stay cable for which the foregoing testing and analysis are aimed, a grouted parallel-bundle cable with two different lengths was considered. The cross section of the cable (Zárate-Brazo Largo Bridges) used in the parametric illustration is composed of 130 parallel 7 mm diameter wires. The steel section of the cable is $\Omega = 0.0050\,\mathrm{m}^2$ and the mass per unit length is $m = 0.059\,\mathrm{tn/m}$. The bending stiffness obtained from the tests as explained further on the paper is $EI = 850\,\mathrm{kN\,m}^2$. The diameter of the composed section (grout and steel) used only to define two different sag/diameter ratios is approximately $\phi = 0.15\,\mathrm{m}$. The cable lengths were selected so as to lead to different sags with the same permanent axial stress $\sigma = 400\,\mathrm{MPa}$ and to the same axial force $N = \sigma\Omega = 2000\,\mathrm{kN}$. The cable is assumed to be of hinged ends, both supports to have the same elevation and the shear deformations negligible in the range of frequencies of interest. The cable sag

Table 1
Natural frequencies of the short cable (Hz)

Order	Straight cable f_n^S	Sagged cable			
		In-plane		Out-of-plane	
		f_n^I	f_n^I/f_n^S	f_n^O	f_n^O/f_n^S
1	1.4302	1.4403	1.0071	1.4302	1.0000
2	2.8647	2.8646	1.0000	2.8647	1.0000
3	4.3079	4.3082	1.0001	4.3079	1.0000
4	5.7639	5.7639	1.0000	5.7639	1.0000
5	7.2371	7.2372	1.0000	7.2371	1.0000
6	8.7315	8.7315	1.0000	8.7315	1.0000
7	10.251	10.251	1.0000	10.251	1.0000
8	11.800	11.800	1.0000	11.800	1.0000
9	13.382	13.382	1.0000	13.382	1.0000
10	15.000	15.000	1.0000	15.000	1.0000

is given by

$$s = \frac{mgL^2}{8N}, \tag{20}$$

while the natural frequencies without sag are given by the closed form expression derived from Eq. (19):

$$f_n = \frac{n}{2L}\sqrt{\frac{N}{m} + \frac{EI}{mL^2}(n\pi)^2}. \tag{21}$$

The first case analyzed corresponds to a short cable with a sag $s = 1\,\phi = 0.15\,\text{m}$ that is obtained according to Eq. (20) with a length $L = 64.4\,\text{m}$. The second case corresponds to a long cable with a sag $s = 10\,\phi = 1.50\,\text{m}$ that is obtained with a length $L = 203.7\,\text{m}$.

Tables 1 and 2 give the natural frequencies of the in-plane and out-of-plane modes for a short cable and for a long one. These natural frequencies were calculated with a numerical model composed of 500 elements of the same horizontal length. The natural frequencies for the straight cable calculated with the numerical model agree with those obtained with Eq. (21), while the natural frequencies of the in-plane modes for the sagged cable obtained with this model agree with the analytical ones presented by Irvine [9]. In Table 1 it can be observed that only the first in-plane frequency is slightly affected by the sag, and none of the out-of-plane ones. Table 2 shows that only the first three in-plane frequencies are modified by the sag while none of the out-of-plane frequencies are modified by the sag.

From these results it follows that the effect of the sag in the out-of-plane frequencies is negligible in both short and long cables typical of the sag/diameter ratios found in cable-stayed bridges.

3. Simultaneous adjustment of the axial force and bending stiffness

A least squares minimization of the following norm is now proposed in order to obtain a balanced adjustment for a set of 20–25 natural frequencies:

$$\sum_n [\tilde{f}_n - f_n^2/\tilde{f}_n]^2 = \text{minimum}, \tag{22}$$

where $\tilde{f}_n$ are the experimentally determined values of the frequencies and f_n are the frequencies of the analytical model. Substituting Eq. (19) in Eq. (22) and multiplying by $(4\pi^2 mL^4)$ one arrives at

$$\sum_n [4\pi^2 mL^4 \tilde{f}_n - NL^2(n\pi - \theta_n)^2/\tilde{f}_n - EI(n\pi - \theta_n)^4/\tilde{f}_n]^2 = \text{minimum}. \tag{23}$$

Table 2
Natural frequencies of the long cable (Hz)

Order	Straight cable f_n^S	Sagged cable			
		In-plane		Out-of-plane	
		f_n^I	f_n^I/f_n^S	f_n^O	f_n^O/f_n^S
1	0.4519	0.4829	1.0685	0.4519	1.0000
2	0.9040	0.9038	0.9997	0.9040	1.0000
3	1.3564	1.3575	1.0008	1.3564	1.0000
4	1.8092	1.8091	1.0000	1.8092	1.0000
5	2.2625	2.2627	1.0001	2.2625	1.0000
6	2.7165	2.7164	1.0000	2.7165	1.0000
7	3.1713	3.1714	1.0000	3.1713	1.0000
8	3.6271	3.6270	1.0000	3.6271	1.0000
9	4.0840	4.0840	1.0000	4.0840	1.0000
10	4.5421	4.5421	1.0000	4.5421	1.0000

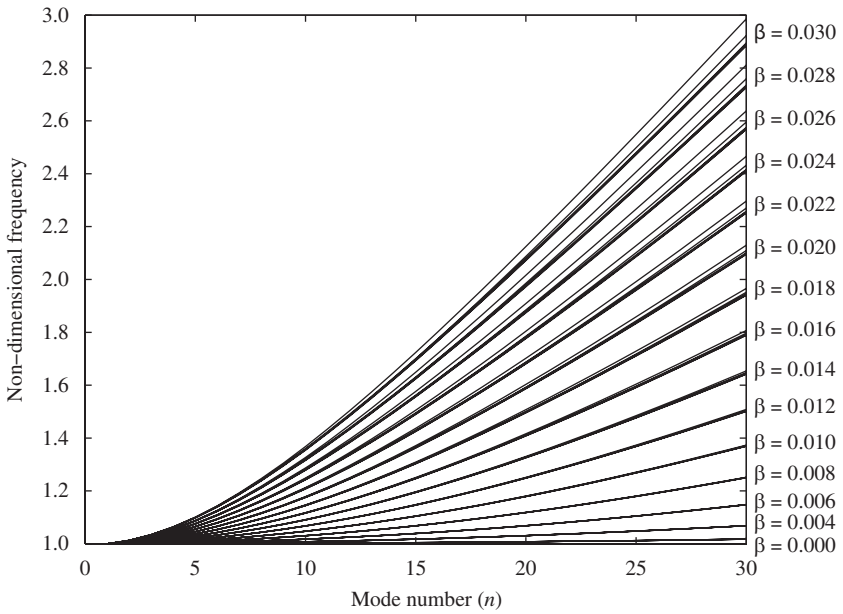

Fig. 1. Progression of non-dimensional frequencies.

The minimizing variables are the axial force N and the bending stiffness EI. The parameters of the rotational stiffness at the cable ends are not included in the list of minimizing variables since the error function is not sensitive to their values. Fig. 1 shows the non-dimensional frequencies $\overline{f}_n$ for given β values and for $k = k_A = k_B$ taking values 0.0, 0.2, 0.4, 0.6, 0.8 and 1.0 with

$$\overline{f}_n = \frac{f_n}{n f_1}, \tag{24}$$

where f_1 is the fundamental frequency assuming hinged ends and n is the order of the mode. The influence of k on the progression of the natural frequencies according to Fig. 1 is only noticeable for relatively large values of β. Therefore, the values of k_A and k_B must be obtained prior to the minimization process as shown in the following section.

Parameter θ_n is a function of both N and EI, although for the purpose of adjustment that dependence is not taken into account. This process is then carried out by iterations to introduce successive corrections in the values of θ_n. The derivatives of Eq. (23) with respect to the minimizing variables N and EI lead to

$$\sum_n [4\pi^2 mL^4 \tilde{f}_n - NL^2(n\pi - \theta_n)^2/\tilde{f}_n - EI(n\pi - \theta_n)^4/\tilde{f}_n](n\pi - \theta_n)^2/\tilde{f}_n = 0, \tag{25a}$$

$$\sum_n [4\pi^2 mL^4 \tilde{f}_n - NL^2(n\pi - \theta_n)^2/\tilde{f}_n - EI(n\pi - \theta_n)^4/\tilde{f}_n](n\pi - \theta_n)^4/\tilde{f}_n = 0. \tag{25b}$$

Equivalently

$$NL^2 \sum_n (n\pi - \theta_n)^4/\tilde{f}_n^2 + EI \sum_n (n\pi - \theta_n)^6/\tilde{f}_n^2 = 4\pi^2 mL^4 \sum_n (n\pi - \theta_n)^2, \tag{26a}$$

$$NL^2 \sum_n (n\pi - \theta_n)^6/\tilde{f}_n^2 + EI \sum_n (n\pi - \theta_n)^8/\tilde{f}_n^2 = 4\pi^2 mL^4 \sum_n (n\pi - \theta_n)^4. \tag{26b}$$

Separating the adjustment variables one arrives at

$$N = 4\pi^2 mL^2 \frac{\sum_n (n\pi - \theta_n)^6/\tilde{f}_n^2 \sum_n (n\pi - \theta_n)^4 - \sum_n (n\pi - \theta_n)^8/\tilde{f}_n^2 \sum_n (n\pi - \theta_n)^2}{(\sum_n (n\pi - \theta_n)^6/\tilde{f}_n^2)^2 - \sum_n (n\pi - \theta_n)^8/\tilde{f}_n^2 \sum_n (n\pi - \theta_n)^4/\tilde{f}_n^2}, \tag{27}$$

$$EI = 4\pi^2 mL^4 \frac{\sum_n (n\pi - \theta_n)^6/\tilde{f}_n^2 \sum_n (n\pi - \theta_n)^2 - \sum_n (n\pi - \theta_n)^4/\tilde{f}_n^2 \sum_n (n\pi - \theta_n)^4}{(\sum_n (n\pi - \theta_n)^6/\tilde{f}_n^2)^2 - \sum_n (n\pi - \theta_n)^8/\tilde{f}_n^2 \sum_n (n\pi - \theta_n)^4/\tilde{f}_n^2}. \tag{28}$$

Convergence of the adjustment variables is found to be quite fast with very small loss of accuracy.

4. Evaluation of the rotational stiffness of the cable ends

The value of the rotational stiffness depends on the configuration of the supports at the cable ends. For the case of cables without deviators or dampers at the ends, a technique to determine that stiffness based on experimental information is proposed and assessed. For cables with intermediate supports between the end anchors in the form of deviators or elastic collars, an analytical procedure based on the geometrical arrangement of the supports, on the magnitude of the axial force and on the bending stiffness of the cable, is proposed in what follows.

4.1. Cables without intermediate supports

The following technique assumes that both cable ends possess identical rotational stiffness $k = k_A = k_B$. The position of the nodes (zero amplitude points) for each mode depends on the bending stiffness β and on the rotational stiffness k. The position of the acceleration sensor used to obtain the cable response during the tests is known, and the order of the lowest mode that presents a node in coincidence with the location of this transducer can be obtained from the Fourier amplitude spectrum of the experimental records. The distance from the bottom end to the first node closer to this end is represented by parameter D. A non-dimensional version of this distance defined as

$$\overline{D} = n\frac{D}{L} \tag{29}$$

is shown in Fig. 2 in function of the mode number and the rotational stiffness for given values of the bending stiffness $\beta = 0.02$ and 0.03. Similar curves for other values of the bending stiffness β, which can be experimentally obtained by means of Eq. (28) for hinged ends, may provide the estimation of the rotational stiffness k for any other cases.

Fig. 3 shows an analytically generated Fourier amplitude spectrum of the free vibrations of a cable with $\beta = 0.02$ for the acceleration sensor located at a distance $D = 0.05\,L$ with respect to the bottom anchor; the lowest frequency that presents a node there is approximately 38 Hz which corresponds to the 22nd mode.

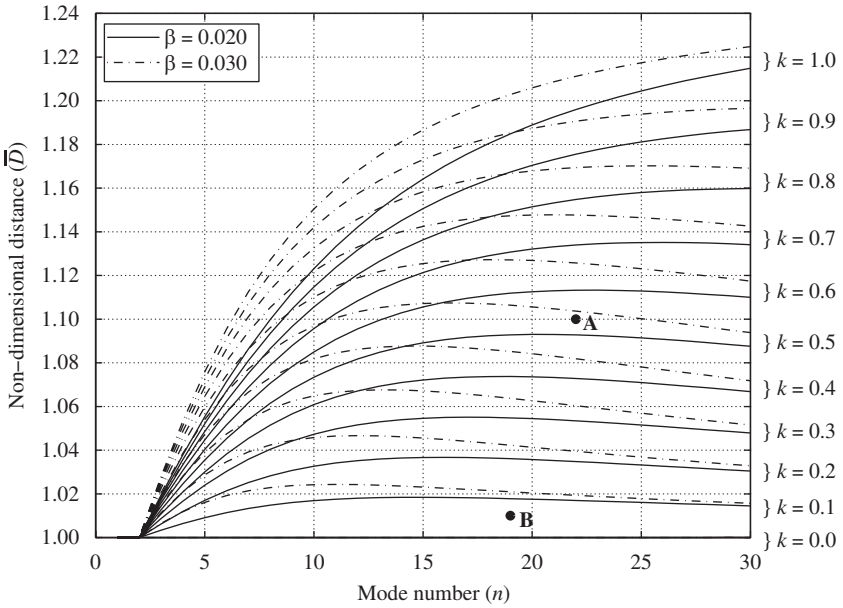

Fig. 2. Position of first nodes for cables with $\beta = 0.020$ and 0.030.

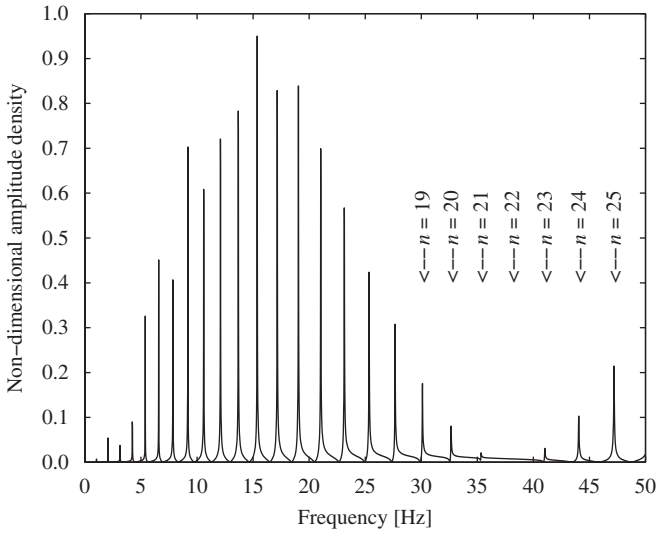

Fig. 3. Analytical FT amplitude density of the acceleration of free vibration of a cable with $\beta = 0.02$ and $k = 0.50$.

For $n = 22$ and $\overline{D} = n\,0.05 = 1.10$, Fig. 2 gives a value of $k = 0.53$ (point A) which is very close to the value $k = 0.50$ used to derive the amplitude spectrum of Fig. 3. The small difference is due to the fact that the value of n would be 21.85 instead of 22 for the given location of the accelerometer. This procedure to determine k turns out to be more accurate for increasing values of β.

Fig. 4 shows a typical spectrum of cable response to the test impact for a cement-grouted parallel-bundle wire cable used in Zárate-Brazo Largo Bridges [6]. This particular cable has a length $L = 52.66$ m and a mass per unit length of $m = 0.1376$ tn/m. The design of these cables is such that the 30 cm of cable at both ends were not grouted with the intention to provide more flexibility and to approximate the hinged condition. Therefore it is not surprising that the equivalent rotational stiffness at the ends as derived with the foregoing procedure is

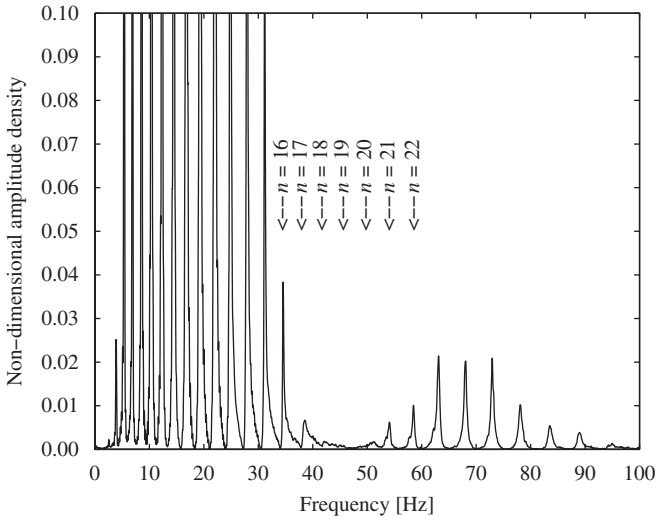

Fig. 4. Typical experimental FT amplitude density of the acceleration of free vibration tests of a cable.

Table 3
Adjusted parameters for an actual cable

Parameter	Experiment	$k = 0.00$	$k = 1.00$
N (kN)	–	2464	2159
EI (kN)	–	5154	4796
β	–	0.0275	0.0283
f_1 (Hz)	–	1.28	1.27
f_2 (Hz)	–	2.58	2.56
f_3 (Hz)	3.90	3.94	3.91
f_4 (Hz)	5.36	5.38	5.35
f_5 (Hz)	6.89	6.92	6.90
f_6 (Hz)	8.57	8.58	8.57
f_7 (Hz)	10.37	10.39	10.38
f_8 (Hz)	12.33	12.35	12.35
f_9 (Hz)	14.47	14.48	14.49
f_{10} (Hz)	16.79	16.78	16.80
f_{11} (Hz)	19.29	19.27	19.29
f_{12} (Hz)	22.00	21.94	21.96
f_{13} (Hz)	24.85	24.81	24.83
f_{14} (Hz)	27.94	27.89	27.90
f_{15} (Hz)	31.17	31.17	31.16

close to zero. This singularity at the ends, however, has been shown to lead to stress concentrations at the cable ends due to dynamic effects at the ends as discussed by Prato and Ceballos in Ref. [7].

Table 3 presents the experimental frequencies adjusted to the hinged end ($k = 0.00$) and fixed end ($k = 1.00$) conditions. This table also gives the axial force and bending stiffness as obtained from Eqs.(27) and (28) for both limiting cases of rotational restraints. The difference in the axial force derived for these conditions is larger than 12 percent even when a good fit between the natural frequencies in both cases is obtained. This result emphasizes the importance of having a good estimate of the rotational stiffness at the ends to achieve an accurate measure of the axial force. In contrast, the bending stiffness β derived for both limiting cases of end restraints does not exhibit appreciable differences, and the value of $\beta = 0.0275$ for the hinged end condition is adequate for the determination of k. The location of the transducer at 2.80 m from the ends detects a node at

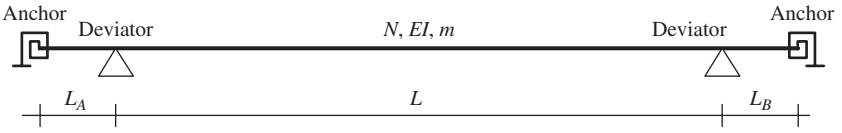

Fig. 5. Model of a cable with intermediate supports.

approximately 45 Hz, which corresponds to the 19th mode (see Fig. 4). The value of non-dimensional distance for $n = 19$ becomes $\overline{D} = 19\,2.80/52.66 = 1.01$. Curves given in Fig. 2 for $\beta = 0.020$ and 0.030 are very close to each other leading to a rotational stiffness $k \approx 0.05$ (point B), which is very close to the hinged condition.

4.2. Cables with intermediate supports

A typical configuration for a cable indicated in Fig. 5 is composed of deviators to distances L_A of the lower anchor and L_B of the upper anchor, without own rotational stiffness, that only restrain the transversal displacement. The influence on the natural frequencies of the degree of fixity of the cable in the anchors decreases with increasing values of the distances L_A and L_B with respect to the length of the cable between the deviators.

The contribution of the spans L_A and L_B in the dynamic behavior of the cable can be represented without precision losses placing rotational springs with frequency dependent dynamic stiffness in correspondence with the deviators. The end conditions that allow determination of constants D_1 to D_4 of the general solution in Eq. (3) for a generic span of length L_0 with hinged end conditions assuming a harmonic unit rotation on the deviators are as follows:

$$u_0 = 0 \quad \text{therefore } D_2 + D_4 = 0, \tag{30a}$$

$$u_{L_0} = 0 \quad \text{therefore } D_1 \sin(\delta L_0) + D_2 \cos(\delta L_0) + D_3 \sinh(\varepsilon L_0) + D_4 \cosh(\varepsilon L_0) = 0, \tag{30b}$$

$$u_0'' = 0 \quad \text{therefore } -\delta^2 D_2 + \varepsilon^2 D_4 = 0, \tag{30c}$$

$$u_{L_0}' = 1 \quad \text{therefore } \delta D_1 \cos(\delta L_0) - \delta D_2 \sin(\delta L_0) + \varepsilon D_3 \cosh(\varepsilon L_0) + \varepsilon D_4 \sinh(\varepsilon L_0) = 1. \tag{30d}$$

The dynamic stiffness of the rotational spring results:

$$K^0 = EI\, u_L'' = EI\, \frac{\sin(\delta L_0)\tanh(\varepsilon L_0)(\delta^2 + \varepsilon^2)}{\varepsilon \sin(\delta L_0) - \delta \cos(\delta L_0)\tanh(\varepsilon L_0)}. \tag{31}$$

The static stiffness that can be utilized for relatively low modes ($n \ll L/L_0$) arises out of the limit of Eq. (31) to $\omega \to 0$:

$$K^0_{\omega\to 0} = \frac{N L_0}{(\coth(\alpha L_0)\alpha L_0 - 1)} \quad \text{with } \alpha = \sqrt{\frac{N}{EI}}. \tag{32}$$

The end conditions for a generic span of length L_0 assumed fixed-hinged are identical to Eq. (30), except that Eq. (30c) should be replaced for

$$u_0' = 0 \quad \text{therefore } \delta D_1 + \varepsilon D_3 = 0. \tag{33}$$

The dynamic stiffness of the rotational spring results in this case:

$$K^1 = EI\, \frac{(\delta \cos(\delta L_0)\tanh(\varepsilon L_0) - \varepsilon \sin(\delta L_0))(\delta^2 + \varepsilon^2)}{2\,\delta\,\varepsilon(\cos(\delta L_0) - \operatorname{sech}(\varepsilon L_0)) + \sin(\delta L_0)\tanh(\varepsilon L_0)(\delta^2 - \varepsilon^2)}. \tag{34}$$

The static stiffness that can be utilized for relatively low modes ($n \ll L/L_0$) arises out of the limit of Eq. (34) to $\omega \to 0$:

$$K^1_{\omega\to 0} = \frac{N L_0(\coth(\alpha L_0)\alpha L_0 - 1)}{\alpha^2 L_0^2 - 2\alpha L_0(\coth(\alpha L_0) - \operatorname{csch}(\alpha L_0))} \quad \text{with } \alpha = \sqrt{\frac{N}{EI}}. \tag{35}$$

One may use the expressions of Eqs. (31) and (34) to define the stiffness of the rotational springs during the adjustment process considering that the values obtained turn out to be similar for growing distances between anchors and deviators. The variability with frequency of the values of rotational stiffness does not present practical difficulties during the application of the recurrence expressions of Eqs. (27) and (28). The dynamic stiffness of these springs becomes null for the frequency of resonance of the span L_0 taking even negative values for greater frequencies. Since the stiffness varies quickly near the resonance it is recommended to adjust low order modes with natural frequencies far away to this resonance to avoid using stiffness estimations with unacceptable errors.

5. Sensitivity of the analysis

In this section special considerations are made regarding influence of different assumptions introduced in the foregoing analysis to determine the axial force.

5.1. Influence of the rotational stiffness at the ends

The work of Geier et al. [5] presents the following approximated expression that provides an estimate of the difference in the axial force of the cable due to the two limiting cases of fixed and free rotations at the ends:

$$\frac{\Delta N}{N} = 4\beta. \tag{36}$$

The linearization that involves Eq. (36) is independent of the order of the mode, although this expression turns out to be strictly applicable only for small values of β. In the present study the following expression obtained considering the simultaneous adjustment of 20 modes of a numerical simulation in Eq. (22) is proposed to extend the validity of Eq. (36) to values of up to $\beta \approx 0.03$:

$$\frac{\Delta N}{N} = 4\beta + 1.5\beta^2 + 1800\beta^3. \tag{37}$$

As an example, the difference in the estimation of the axial force of a cable such as that reported in Ref. [5] for $\beta_{\max} \approx 0.01$ turns out to be $\Delta N/N \approx 4$ percent, while for the cables of the Zarate-Brazo Largo Bridges for $\beta_{\max} \approx 0.025$ it goes up to $\Delta N/N \approx 12$ percent.

5.2. Influence of the shear flexibility and rotational inertia

Grouted parallel-bundle cables which are the focus of this work may be regarded as slender composite section beams where the cement grout contributes very significantly to the overall bending stiffness of the cable. As such, the influence of the shear flexibility of the composite section in the natural frequencies may become significant for higher modes such as those excited and measured in the proposed experimental procedure, even though it is beyond discussion that such modes are not relevant for the behavior of the cables under typical loads acting on the stay cables of a bridge. The subject is only brought into attention in order to assess the effect of the shear flexibility of the composite cable cross section in the higher natural modes excited in the tests by the impulsive test loads.

The authors have not found in the literature a discussion of the influence of the shear flexibility and the rotational inertia on the progression of the natural frequencies of the cable. The effect of the bending stiffness can be appreciable since the lowest natural frequencies while the shear flexibility and the rotational inertia have a larger incidence in higher modes. A convenient alternative to limit the influence of these parameters consists of defining a maximum number of modes to consider during the adjustment process. Such maximum number is derived from the differential equation taking into account the transverse shear flexibility and the rotational inertia as in [8]

$$EI\,u^{\mathrm{iv}}(x)\,y(t) - N\,u''(x)\,y(t) + m\,u(x)\,\ddot{y}(t) - m\left(\frac{EI}{GA_c} + r^2\right)u''(x)\,\ddot{y}(t) + \frac{m^2r^2}{GA_c}u(x)\,\dddot{y}(t) = 0, \tag{38}$$

where GA_c is the shear stiffness constant and r is the radius of gyration of the cross section. In order to capture the influence of these parameters on the natural frequencies only the hinged end condition of available analytical resolution is considered. The modal shapes associated with a cable hinged at the two ends are

$$u(x) = \sin\left(\frac{n\pi}{L}x\right). \tag{39}$$

Substituting Eq. (39) in Eq. (38) with $y(t) = e^{i\omega t}$, one arrives at

$$EI\left(\frac{n\pi}{L}\right)^4 + N\left(\frac{n\pi}{L}\right)^2 - m\omega^2 - m\omega^2\left(\frac{EI}{GA_c} + r^2\right)\left(\frac{n\pi}{L}\right)^2 + m^2\omega^4\frac{r^2}{GA_c} = 0. \tag{40}$$

The last term of Eq. (40) originates from the coupling of shear deformations and rotational inertia only affects the higher modes where the influence of direct terms is preponderant. The natural frequencies neglecting this term are obtained by the expression

$$\hat{\omega}_n = 2\pi\hat{f}_n = \frac{n\pi}{L}\sqrt{\frac{N}{m}}\sqrt{\frac{1+\beta^2 n^2\pi^2}{1+\left(\frac{EI}{GA_cL^2}+\frac{r^2}{L^2}\right)n^2\pi^2}}. \tag{41}$$

Assuming steel cables with a solid circular cross section,

$$E = 2.6G, \tag{42a}$$

$$A_c = 0.9A, \tag{42b}$$

and thus

$$\left(\frac{EI}{GA_cL^2} + \frac{r^2}{L^2}\right) \approx \frac{4}{\lambda^2}, \tag{43}$$

where

$$r = \sqrt{\frac{I}{A}}, \tag{44a}$$

$$\lambda = \frac{L}{r}. \tag{44b}$$

Eq. (41) then becomes

$$\hat{\omega}_n = 2\pi\hat{f}_n = \frac{n\pi}{L}\sqrt{\frac{N}{m}}\sqrt{\frac{1+\beta^2 n^2\pi^2}{1+4\pi^2 n^2/\lambda^2}}. \tag{45}$$

The denominator of the last root of Eq. (45) represents the effect of the shear deformations and rotational inertia, which becomes more significant as the order mode n increases and the slenderness λ decreases. As an example, to attain an error bound of 1 percent in the estimation of the axial force, a maximum error of 0.5 percent must be warranted in the natural frequency:

$$(f_n - \hat{f}_n)/\hat{f}_n \leqslant 0.005, \tag{46a}$$

$$\sqrt{1+4\pi^2 n^2/\lambda^2} - 1 \leqslant 0.005. \tag{46b}$$

Then

$$n \leqslant 0.01594\,\lambda. \tag{47}$$

From a practical point of view it is not convenient to take more than 25 or 30 modes. Eq. (47) gives then the maximum number of modes that could be considered in the analysis of the experimental results to limit the influence of the shear deformations and rotational inertia. The cables of the Danube Channel Bridge [5] have a slenderness of about $\lambda \approx 3000$ ($n = 50$). In contrast, the largest slenderness ratio of the cables of the

Zarate-Brazo Largo Bridges [6] turns out to be $\lambda_{max} \approx 7000$ ($n = 110$) while the minimum slenderness is only $\lambda_{min} \approx 1500$ ($n = 25$).

5.3. Influence of the transverse stiffness of the intermediate supports

Casas [1] considers that the definition of the effective length of the cable for the case of complex anchor devices can result in a critical aspect in determining the axial force. Geier et al. [5] propose to measure the distance among nodes of high modes near the ends to calculate then the effective length as the product of this distance by the order of the corresponding mode. In the case of cable with relatively flexible intermediate supports one can obtain acceptable precision in the estimation of the axial force by applying adjustment techniques typical of experimental modal analysis, as proposed by Kim and Park [10], with both rotational and translational springs.

6. Conclusions

A procedure to obtain the axial force acting on a cable from free vibration tests has been presented. The proposed experimental procedure is a simple, reliable and easy to apply method that can readily be carried out with a single accelerometer to record the response to a hand-induced impulse applied near the cable ends in the horizontal direction normal to the vertical plane of the cable. In this way estimation of the cable force becomes independent of the elastic axial stiffness and of the sag of the cable. The proposed adjustment procedure does not require mobilizing appreciable response of the fundamental mode since the higher modes used in the optimization scheme may be more easily excited close to the cable ends.

In contrast to recent work [10] on the subject where numerical models are used, here the analysis is carried out as in earlier references [1–5] through analytical solutions, and the axial force is derived by optimizing the correspondence between measured and analytical natural frequencies considering as simultaneous adjustment variables the axial force and the bending stiffness of the cable. It is shown that the influence of the rotational stiffness at the cable ends on the estimation of the axial force increases with the bending stiffness of the cable and thus it is of special interest in the case of grouted parallel-bundle wire cables of proportions typical of existing cable-stayed bridges.

The natural frequencies of a cable with elastic rotations restraints at the ends has been derived in an explicit form as given in Eq. (19), although its application to derive the value of the axial force on the cable requires an iterative sequence since parameter θ is a function of the natural frequency itself unless the cable is doubly hinged at the ends. For cables with deviator collars near the ends an analytical solution is proposed to derive the rotational stiffness at the supports, while an experimental procedure is proposed for the case of cables without deviators. The effect of the rotary inertia and shear stiffness of the study cables is found not to affect the estimation of the axial force as long as the number of modes used is limited to the lowest 20–25 modes.

Acknowledgments

The present work was carried out with support from the National Research Council of Argentina (CONICET). The tests of the Zárate-Brazo Largo Bridges were possible by an agreement between the National University of Córdoba (UNC) and the National Highway Directorate of Argentina (DNV).

References

[1] J.R. Casas, A combined method for measuring cable forces: the cable-stayed Alamillo Bridge, Spain, *Structural Engineering International, IABSE* 4 (4) (1994) 235–240.

[2] W.-X. Ren, G. Chen, W.-H. Hu, Empirical formulas to estimate cable tension by cable fundamental frequency, *Structural Engineering and Mechanics—An International Journal* 20 (3) (2005) 363–380.

[3] S.W. Smith, M. Johnson, Field test to determine frequencies of bridge stay cables, *Proceedings of the XVII International Modal Analysis Conference*, Kissimmee, Florida, February 1999, pp. 745–751.

[4] S.W. Smith, J.E. Campbell, Testing and model verification of the Maysville Kentucky Bridge stay cables, *Proceedings of the XX International Modal Analysis Conference*, Los Angeles, California, February 2002, pp. 1050–1056.
[5] R. Geier, G. De Roeck, J. Petz, Cable force determination for the Danube Channel Bridge in Vienna, *Structural Engineering International, IABSE* 15 (3) (2005) 181–185.
[6] C.A. Prato, M.A. Ceballos, P.J.F. Huerta, C.F. Gerbaudo, C.E. Grünbaum, D.L. Hommel, Diagnosis, construction procedures and design recommendations for replacement of cables in cable-stayed bridges: experience from two current cases in Argentina, *US–Canada–Europe Workshop on Bridge Engineering: Recent Advances in Bridge Engineering*, Zurich, Switzerland, July 1997, pp. 303–316.
[7] C.A. Prato, M.A. Ceballos, Dynamic bending stresses near the ends of parallel-bundle stay cables, *Structural Engineering International, IABSE* 13 (1) (2003) 64–68.
[8] R.W. Clough, J. Penzien, *Dynamics of Structures*, McGraw-Hill, New York, 1993.
[9] H.M. Irvine, *Cable Structures*, MIT Press, Cambridge, MA, 1981.
[10] B.H. Kim, T. Park, Estimation of cable tension force using the frequency-based system identification method, *Journal of Sound and Vibration* 304 (3–5) (2007) 660–676.